
Geomagnetic Storms

Most operational systems can withstand certain levels of disturbances in the magnetosphere and ionosphere, but large geomagnetic storms can cause deleterious effects on space- and ground-based installations. The manifestations of storms are strong deviations in the Earth's magnetic field from the quiet conditions that extend over wide geographic areas: from high-latitude to mid-latitude and equatorial regions. Significant geomagnetic disturbances produce awe-inspiring auroral displays (designated aurora borealis in the northern hemisphere and aurora australis in the southern hemisphere), which have attracted the interest of generations of scientists, but they can also cause disruptive effects such as loss of satellites and failure of communications networks and electric power grids.

The disturbances in the geomagnetic fields are caused by fluctuations in the solar wind impinging on the Earth. The disturbances may be limited to the high-latitude polar regions, unless the interplanetary magnetic field (IMF) carried by the solar wind has long periods (several hours or more) of southward component ($B_z < 0$) with large magnitudes (greater than 10-15 nT). The occurrence of such a period stresses the magnetosphere continuously, causing the magnetic field disturbances to reach the equatorial region. The degree of the equatorial magnetic field deviation, the measure of the magnitude of geomagnetic storms, is usually given by the Dst index. This is the hourly average of the deviations of the H (horizontal) component of the magnetic field measured by several ground stations in mid- to low-latitudes. Dst = 0 means no deviation from the quiet condition, and Dst < -100 nT means large storms. During the March 1989 storm that caused the province-wide blackout in Quebec, Canada, the Dst index reached approximately -600 nT.

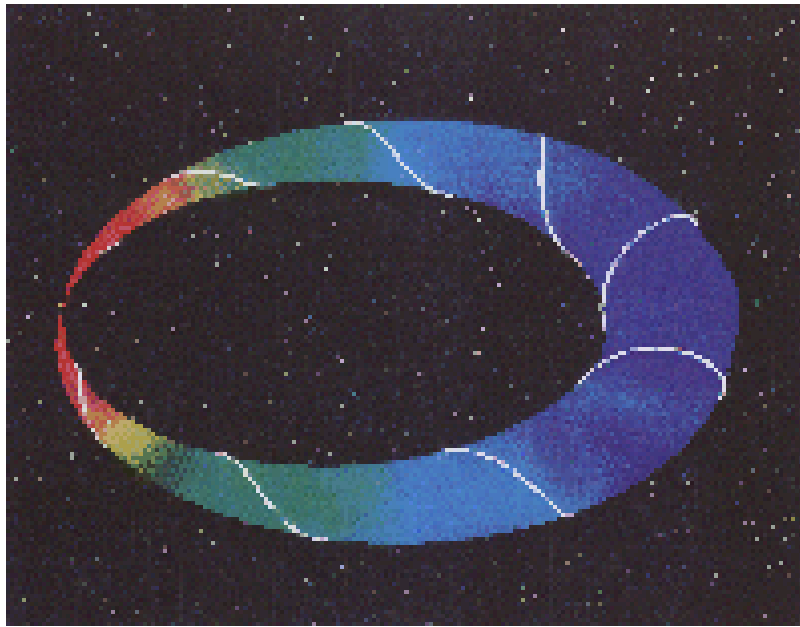
There is another type of storms. These recur with periods of approximately 27 days, the solar rotation period, and are associated with the high-speed solar wind originating in "coronal holes" at the Sun. Such storms tend to be moderate. Severe storms tend to be nonrecurrent and are difficult to predict.

Geoeffective Conditions: What Causes Geomagnetic Storms?

Large geomagnetic storms are usually caused by structures in the solar wind having specific features: long durations of strong southward interplanetary magnetic field (IMF) impinging on the Earth's magnetosphere. These features are effective in causing geomagnetic disturbances and are said to be geoeffective. We use the term geoeffective to mean "storm-causing," with the resulting storm severity exceeding a specified threshold. Currently, the criterion is that Dst remain below -80 nT for two hours or longer. Geoeffective solar wind structures are clearly distinguishable from the typical solar wind characterized by weak (typically 5 nT) fluctuating IMF. They can be described as magnetic flux ropes, often referred to as magnetic clouds (Burlaga, 1988), and are highly correlated with coronal mass ejections (CMEs), an eruptive solar phenomenon in which enormous amounts of plasma (10^{15} g) and magnetic energy (10^{32} - 10^{33} erg) are ejected by the Sun at high speeds reaching several hundred to more than 1000 kilometers per second. The sporadic eruptions and the subsequent propagation of the ejecta cannot be predicted accurately at this time. The storm prediction techniques currently in use, which rely on observations of solar activity, can provide forecasting time of a few days but are not accurate [Joselyn, 1995].

The new prediction method takes advantage of the distinct physical attributes of geoeffective solar structures in the following way. (1) They are magnetically well organized, so that the leading edge of a structure has clear relations to the solar wind that has yet to arrive at the observing platform. (2) The long durations of the solar wind drivers of large storms can provide forecasting time, in the range of several hours to more than 20 hours, depending, among other factors, on the solar cycle.

Theoretical model of a magnetic cloud.

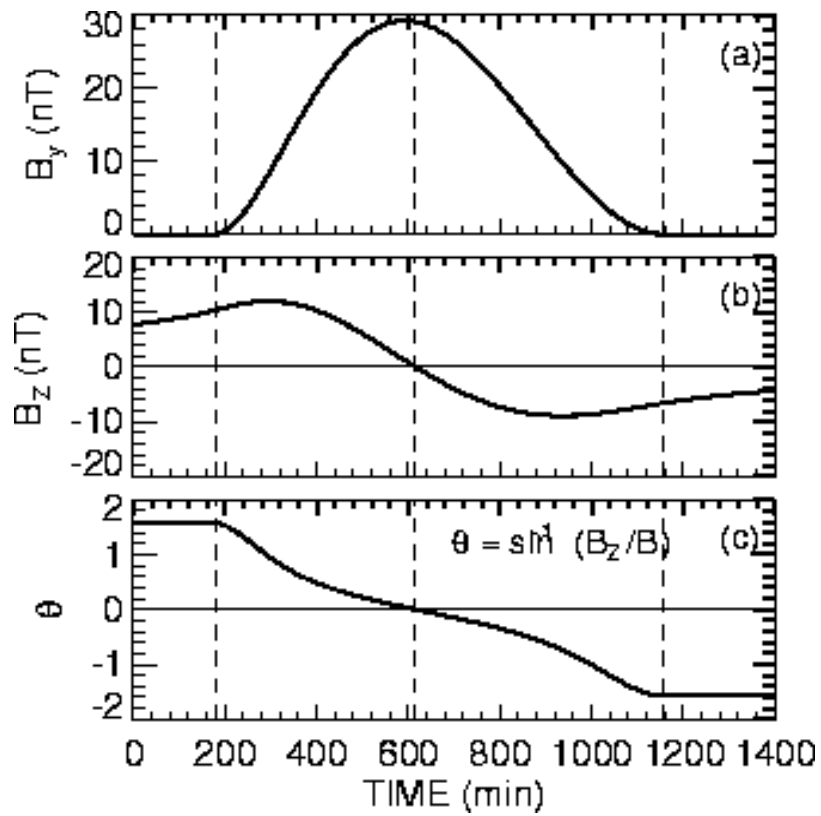


A solar flux rope propagating toward the Earth (the green asterisk on the right) from the Sun (on the left). (Figure from Chen et al. [1995]. See [Chen \[1996\]](#) for the theory.) The dimensions of the model flux rope are shown to scale in relation to the Sun-Earth distance (1 AU). The color scheme shows the average magnetic field strength, ranging from strong (red, of the order of a gauss) to weak (blue, of the order of 10 nT). The helical curve illustrates a characteristic magnetic field line. Magnetic clouds may indeed be structurally simple as depicted here. Recent observations indicate that magnetic field lines of magnetic clouds do remain connected to the Sun and that the field lines toward the outer edge of a flux rope are more twisted [[Larson et al., 1997](#)]. This property is implied by the model structure and the magnetic field described below.

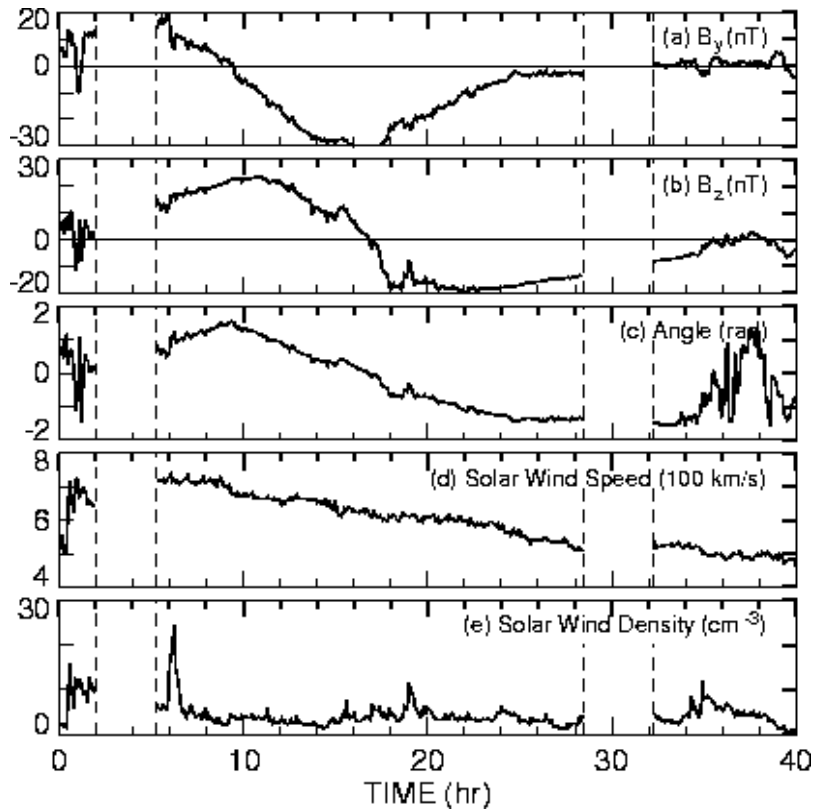
Click [here](#) to view the time evolution of the magnetic cloud.

Magnetic field profile associated with the above model magnetic cloud.

As the model magnetic cloud moves past the Earth, an observer (e.g., a satellite) sees a magnetic field varying in time. In this example, the northward component ($B_z > 0$) arrives at the Earth first [adapted from [Chen \(1996\)](#)]. The continued expansion in the minor radial direction is taken into account. Although no ambient magnetic field is included outside the cloud edges (the vertical dashed lines), the solar wind typically has fluctuating field of roughly 5 nT in magnitude. A nonzero B_y outside the flux rope will cause theta (panel c) to decrease.



An interplanetary magnetic cloud observed by IMP 8 on 13-14 January 1988.



The B_y and B_z components and θ are shown. The above theoretical model closely resembles the observed magnetic cloud. The B_y component, which is in the east-west direction, peaks where $B_z = 0$. The sign difference in B_y between the model and the observed cloud is insignificant. The solar wind speed V and density are also shown. Two major gaps in the data are indicated by vertical dashed lines.

A Feature-Based Method of Predicting Geoeffective Solar Wind and Geomagnetic Storms

This technique takes advantage of the fact that the solar wind (SW) features that cause large storms, long uninterrupted durations of strong southward or northward magnetic field, make such geoeffective structures clearly distinguishable from the nongeoeffective ("background") solar wind. They can be described as magnetic flux ropes propagating past the Earth. If the magnetic field of an interplanetary flux rope is measured, the field vector shows a characteristic rotation which is much slower than the time scale of IMF fluctuations in the background solar wind. The slow rotation of the magnetic field can be recognized and used to infer the magnetic field profile of the solar wind that has yet to arrive at the Earth. This means that the leading edge of the SW structure has a structural relationship to the trailing edge. The basic technique falls under the broad category of artificial intelligence. Another artificial intelligence approach uses neural networks, and a number of neural network space weather forecasting techniques are under development elsewhere. The basic difference is that our technique seeks to estimate the magnetic field profile (B_z) forward in time, in the solar wind that has yet to arrive at the observing platform. The response of the magnetosphere to the predicted B_z profile is then inferred. In contrast, the neural network approach attempts to predict the response of the magnetosphere to the solar wind that has been observed.

Because the Earth passage of magnetic clouds takes 10-20 hours to a few days, the method allows prediction of IMF forward in time. As a result, the method can yield advance forecasting time of several to more than 10 hours. This is far in excess of the warning time achieved by the current neural network techniques which attempt to predict the response of the magnetosphere to the measured solar wind data. (See [Chen et al. \[1996, 1997\]](#) for more detail.)

Test Criteria and Dst Threshold

The test is being conducted to examine the degree of success one can expect from the method in its present form with respect to the following specific objectives. The first is to estimate the eventual duration τ and maximum value of B_z field (denoted B_{zm}) of each solar wind event being encountered. The second objective is to estimate the $B_z(t)$ profile of the solar wind stream that has yet to come. The third objective is to determine whether the event is geoeffective or not geoeffective according to the estimated B_{zm} and τ . The threshold for geoeffectiveness is chosen to be $Dst < -80$ nT for two hours or longer. Our overall objective is to accurately identify and predict the solar wind events that cause large geomagnetic storms rather than the detailed response of the magnetosphere. We judge the success of the technique as follows. If a solar wind event leads to $P1 > 0.5$ for 2 hours or longer, we regard the outcome as a positive prediction of the occurrence of $Dst < -80$ nT. We then compare this outcome with the actual or provisional Dst value, whichever may be available. If Dst does fall and remain below this threshold for two hours or longer, the prediction is judged to be correct. If $P1$ does not exceed 0.5 for two hours or longer but Dst does fall below the -80 nT threshold, then the result is judged to be a false negative (a miss). If $P1$ produces a positive prediction for storm but Dst does not fall below the -80 nT threshold, the outcome is judged to be a false positive (a false alarm). The association between the solar wind events and the Dst values can be subjective, but we generally do not encounter obvious ambiguity.

References

1. Burlaga, L. F., Magnetic clouds and force-free fields with constant α , *J. Geophys. Res.*, 93, 7217, 1988.
2. Chen, J., and D. A. Garren, Interplanetary magnetic clouds: Topology and driving mechanism, *Geophys. Res. Lett.*, 20, 2319, 1993.
3. Chen, J., P. J. Cargill, and S. P. Slinker, Plasma Physics of Solar-Terrestrial Coupling, *1995 NRL Review*, NRL/PU/5230--95-274 May 1995.
4. Chen, J., Theory of prominence eruption and propagation: Interplanetary consequences, *J. Geophys. Res.*, 101, 27,499, 1996.
5. Chen, J., P. J. Cargill, and P. J. Palmadesso, Real-time identification and prediction of geoeffective solar wind structures, *Geophys. Res. Lett.*, 23, 625, 1996.

6. Chen, J., P. J. Cargill, and P. J. Palmadesso, Predicting solar wind structures and their geoeffectiveness, *J. Geophys. Res.*, *102*, 14701, 1997.
7. Joselyn, J. A., Geomagnetic activity forecasting: The state of the art, *Rev. Geophys.*, *33*, 383, 1995.
8. Larson, D. E., et al., Tracing the topology of the October 18-20, 1995, magnetic cloud with 0.1-100 keV electrons, *Geophys. Res. Lett.*, *24*, 1911, 1997.